Optical remote sensing Practice 2

EARTH OBSERVATION PRACTICAL

Instructor: Stien Heremans
Group number:14
Group members: Lien De Trift, Shima Karimi, Zhiqi Wang
Date: 24/12/2021

1. Introduction

Some landcover types, such as urban forests, shrubs, even gardens, and other vegetation types in urbanized cities, can provide a range of ecosystem services to citizens. Some examples are air purification, urban temperature regulation, noise reduction, and runoff reduction. Although these examples are all positive, some changes in landcover can also lead to ecosystem disservices such as air pollution, inclusively allergies, and infrastructural damage. The impacts can be tangible on an ecological, economic, and social scale. In this report, the link between landcover and the air quality concept will mainly be handled. It has been scientifically proven by many studies that urban forests help in reducing air pollution levels and offset greenhouse gas (GHG) emissions in cities (Baró et al., 2014).

Many researchers have already tried to examine the air quality in Flanders. High-resolution data is not available for every place in the world. Therefore, the combination of model results and available measurement data makes it possible to assess the air quality at a local scale. Maps of air quality show that almost 35% of the population in Flanders is exposed to daily PM_{10} concentrations higher than 50 $\mu g/m^3$ (Lefebvre et al., 2011). Another more recent study is "CurieuzeNeuzen". This project, raised through crowdsourcing and in cooperation with KU Leuven, gathered a high proportion of high-quality measurements that led to a map of the nitrogen dioxide concentrations in the air all over Flanders. It shows that air quality is not only a problem in the big, urbanized cities but also in the small villages (De Craemer et al., 2020). This problem is still a major challenge in Flanders. To control and improve air quality in the future, an understanding of the main drivers of air pollution is necessary (Meysman & De Craemer, 2018).

The first optical report aimed to explore and preprocess Sentinel-2 satellite hyperspectral and multispectral data from winter and summer. The second part of the assignment proceeds with the stacked images from Brussels and focuses on the classification of these winter and summer images. The first goal is to get insight into different classification algorithms and the accuracy assessment. In this report, only two main classification methods are described and discussed for both images: the unsupervised and supervised classification methods. Based on an accuracy assessment, the 'best product' will be used to determine the air quality and its link with landcover in the area. Because the study area of Brussels is quite large, three focus regions with a different dominant landcover type will be compared. To get insight into the temporal drivers, a comparison will also be made between the summer and winter data. To conclude, the final goal of this assignment is to link air quality in Brussels to spatial and temporal drivers such as the landcover type and how they seasonally change in the highly urbanized and developed city.

2. Material & Methods

The image classification, accuracy assessment, and air quality analysis were carried out with QGIS 3.10 software. An entirety of algorithms exists for image classification purposes. Specifically, the Semi-Automatic Classification Plugin (SCP) was chosen to carry out the supervised classification.

The main principle of image classification is the distribution of the different pixels into a different class based on the spectral properties of that pixel. The comparison of the different pixels was done by an algorithm that sorts them into a defined range of possible landcovers. The result of this classification is a map, containing a mosaic of pixels that are attributed to a particular landcover class depending on its spectral reflectance characteristics.

In general, there exist two different methods of image classification. In this report, the unsupervised classification method was performed followed by the supervised classification method. Both methods were done using different criteria. The accuracy assessment was checked for each criterion in order to find the 'best' classified image, required in further air quality investigation.
The preprocessed Sentinel-2 winter and summer TOA 9-band images (band 2, 3, 4, 5, 6, 7, 8a, 11, 12) were selected for the classification as these were, as mentioned in the previous report, better in distinguishing some features in the landscape.

2.1. Unsupervised Classification

The unsupervised classification method, unlike the supervised classification, does not require any training data, and it is entirely carried out in an automated way. In this method, each individual pixel is assigned to a class without any prior knowledge about the definition of that class. The algorithms group together pixels that are related in a cluster. The user only must define the number of clusters that are assumed necessary, and which bands to use, but there is no reliance on training data screened by the user. After classification, the cluster map must be validated with available reference data to identify the present classes or clusters. This method can be used to determine the possible classes, but further detailed analysis is required (Walton et al., 2015).

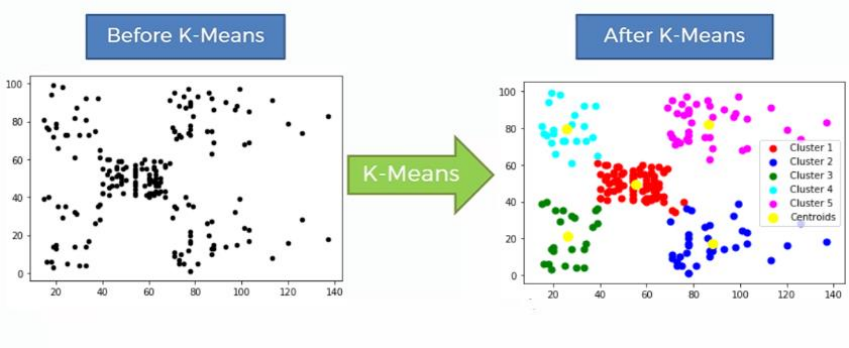

Figure 1: Unsupervised classification method illustrated with 5 clusters (Singh, 2020).

There are numerous tools available in QGIS that analyze the spectral curve of each pixel and that separate them into different clusters based on this spectral separability. For our case, the K-means clustering grid tool was used. This method, as described in Figure 1, classifies each pixel based on the comparison of each pixel value with the nearest mean, represented as one cluster (Figure 1) (Singh, 2020). Different classifications were performed on the summer and winter images according to different criteria. First, the three possible methodologies were applied, namely Iterative Distance (Forgy, 1965), Hill-Climbing (Rubin, 1967), and an algorithm that is a combination of those two methods. Next, different classifications were done with the 'best' method, but changing the number of clusters to respectively 5, 10, and 20. Finally, the number of iterations was tested in order to see the implication of this setting on the classification map.

2.2. Supervised Classification

The second classification method does require more input from the user, unlike the unsupervised classification method. Therefore, the methodology is also more complex, and the process is divided into three different stages: the training stage, the classification stage, and the output stage. In the training stage, a group of training pixels (= training areas) are selected to train the model, and which are associated with each class. These training areas must be chosen in such a way, so they cover a

large enough homogeneous area, and they are representative. Additionally, the number of pixels in a training polygon must be sufficient to consider also local variations. In the classification stage, each pixel is classified based on the spectral signatures from these training areas to the class it most closely resembles. This is done by an algorithm. In the third step, the output stage, results are shown, and the accuracy is analyzed (Figure 2).

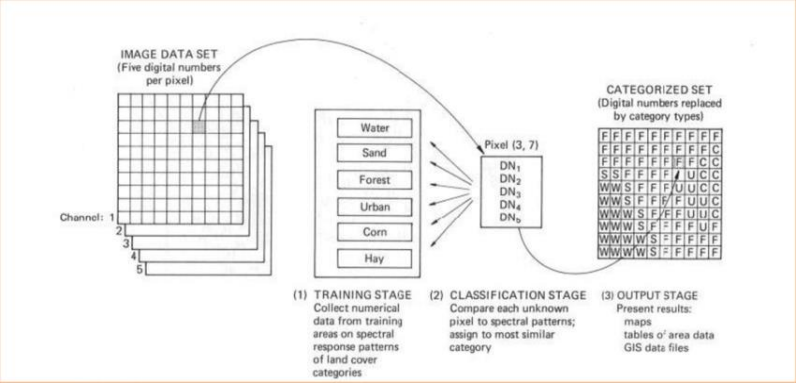

Figure 2: Illustration of the three basic stages in the supervised classification method (Alkhouri, 2015).

The unsupervised classification method was carried out for the winter and summer images, using the Semi-Automated Classification Plugin (SCP) in QGIS. The training areas, used to identify landcover classes based on different spectral curves, were created based on the available LC shapefiles (LC_calibration, LC_validation) by Vebros et al., (2017). In total, four general landcover classes were distinguished: including water, urban, vegetation, and soil. Some landcover classes, especially the urban landcover class, could be further specified in numerous subclasses. Table 1 gives an overview of the different macro classes and subclasses, each indicated with an ID (Table 1). For the summer image, bare soils were not considered, as they are usually not present in summer.

Table 1: Landcover macro classes (MC ID) and subclasses (C ID).

Macro class ID (MC ID)	Macro class name	Subclass ID (C ID)	Subclass name
0	Unclassified	0	Unclassified
1	Urban	1	Continuous urban fabric
		2	Discontinuous dense urban fabric
		3	Discontinuous medium density urban fabric
		4	Discontinuous low density urban fabric
		5	Industry
		6	Road
		7	Railway
2	Arable land	8	Arable land
3	Forest	9	Forest
4	Grassland	10	Green urban area
5	Water	11	River
6	Bare soil	12	Bare soil

In the classification algorithm itself, different methods were selected to assign each pixel to a class. The “Minimum Distance Classifier” assigns the pixel to the class that is closest to the vector space of that class. The “Maximum Likelihood classifier” attributes the pixel to the class that has the highest statistical probability of being part of that class. The last method, “Spectral angle mapping”, puts the pixel in the class where the angle between that class and the pixel is the smallest (Perumal & Bhaskaran, 2010). For each image, the different methodologies were tested.

2.3. Accuracy Assessment

The accuracy assessment was also performed through the SCP to be able to choose the best final classification product required in the air quality application. This part of the classification, where the classified image is compared with reference data, is indispensable. The accuracy assessment consists of two steps, namely the generation of validation data and the calculation of the accuracy matrix. The creation of the validation data was done by making a new shapefile and drawing the polygons by hand in QGIS. The accuracy was quantified by comparing the validation data set to the classified data. The output is an error matrix, where the diagonal elements represent the correctly classified pixels in reference to the validation data. Logically, the non-diagonal elements represent the pixels that were put in an incorrect class.

Different measures were considered during the accuracy assessment. First, the Producer's Accuracy was calculated as the number of correctly classified pixels of one class divided by the total reference pixels of that class. The result is a percentage representing the probability that a pixel will be classified correctly. Next, the User's Accuracy (UA) is the ratio of the pixels classified in a class and the total pixels classified in that class (Humboldt State University, 2019). The Kappa coefficient, known as kappa hat, was also given as a statistical measure to evaluate the classification's accuracy. Kappa hat evaluates whether the classification is better compared to the random and is expressed in a value between -1 and 1 (Humboldt State University, 2019).

2.4. Application: air quality in Brussels

Finally, the air quality in Brussels was assessed based on the most accurate classification map according to the accuracy assessment. To achieve this, a qualitative air quality score was needed to be defined for each land use class. The scores were assigned to each class based on a study from VITO (2018). Also, the maximum particulate matter depositions values PM_{10} were given per land cover class (in kg/ha) (Table 2).

Table 2: PM_{10} qualitative scores and maximal deposition (kg/ha) for different land cover classes (VITO, 2018)

Land cover	*Qualitative score*	*Maximal deposition [kg/ha]*
Coastal habitat without vegetation	1	0
Coastal habitat with low vegetation	3	36
Coastal habitat with forest vegetation	6	73
Grasslands	3	36
Deciduous forest	7	88
Coniferous forest	10	127
Heathlands	3	36
Water	1	0
Marshland	3	36
Rivers	1	0
Meadows	3	36
Arable land	2	12
Urban	1	0

The scores and values were calculated using the raster calculator for the winter and the summer images. It assigns the scores based on the present landcover classes, and consequently the maximum PM_{10} deposition values for each pixel. For forest landcover, a value of 7 was chosen, as deciduous trees are most dominant in the study area. Bare soils are treated as urban land and receive a qualitative value of 1, and a quantitative value of 0. The chosen values for the landcover classes of water, urban, grassland, arable land, and bare soil are straightforward.

Finally, the mean and maximum values for both the scores and depositions were calculated within the three focus regions A, B, and C using the Zonal Statistics tool in QGIS. The calculations were again performed for both the summer and winter images to get insight into the influence of landcover and season on the air quality in the three regions.

3. Results

3.1. Unsupervised Classification

Figure 3 shows the unsupervised classification maps carried out for the three different methods using 5 clusters and 10 iterations: Iterative Minimum Distance, Hill-climbing, and the combination of both, and an increase in the number of iterations (10, 20, 50). First, the increased number of iterations did not affect the quality of the classification, but only had an impact on the total calculation time. The influence of the methodology on the classification outcome is determined on the winter images. Both methods do not accurately represent the actual land cover in the study area. It is difficult to identify the class name of each color. Although the classification is not optimal, the most relevant unsupervised classification method seemed to be the combination of Iterative Minimum Distance and Hill-Combining methods. Here, the water bodies are more or less classified as a separate class, but there is still a lot of confusion between the urban and forest land cover class (Figure 3).

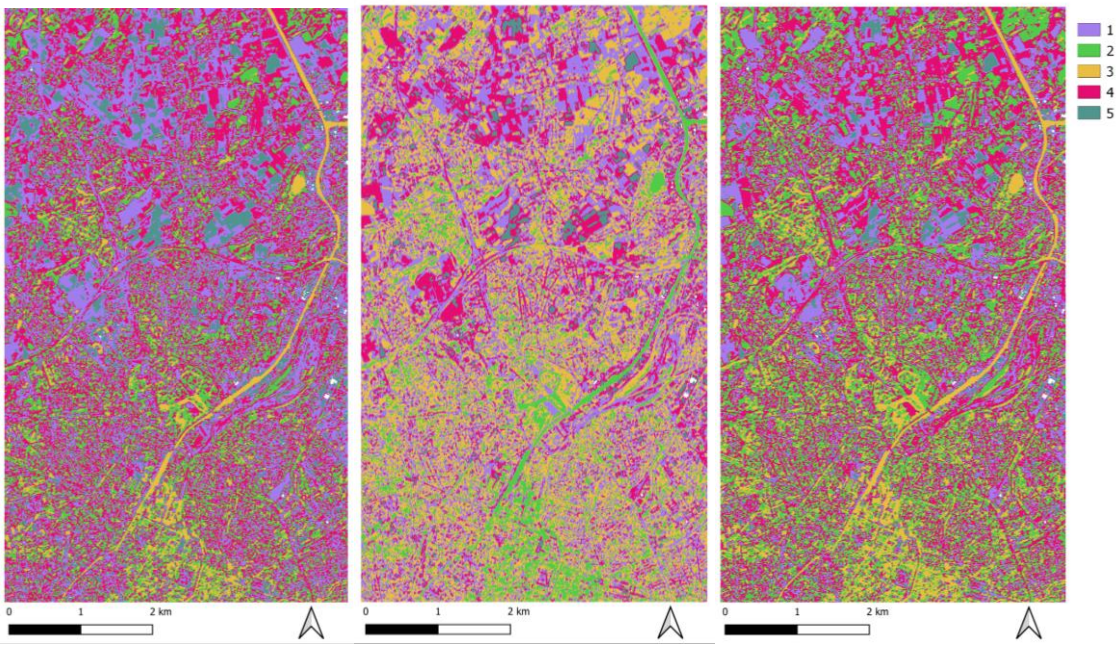

Figure 3: Unsupervised classification maps for winter using different methods; left: IMD, middle: HC, right: CMD.

For the summer images, the influence of the number of clusters on the classification is represented (Figure 4). The classification method Iterative minimum distance was used both for 5 classes, 10 classes, and 20 classes and a choice of 10 iterations each. It is clear that a higher number of clusters increases the level of detail but makes it more difficult to distinguish the different landcover classes. The map with 5 clusters seems to have the best classification result, although the water bodies are not visible in the land cover map. A guess of the present land covers could be the following: forest (dark green), arable land (red), grassland (yellow), urban (purple), industry (light green) (Figure 4).

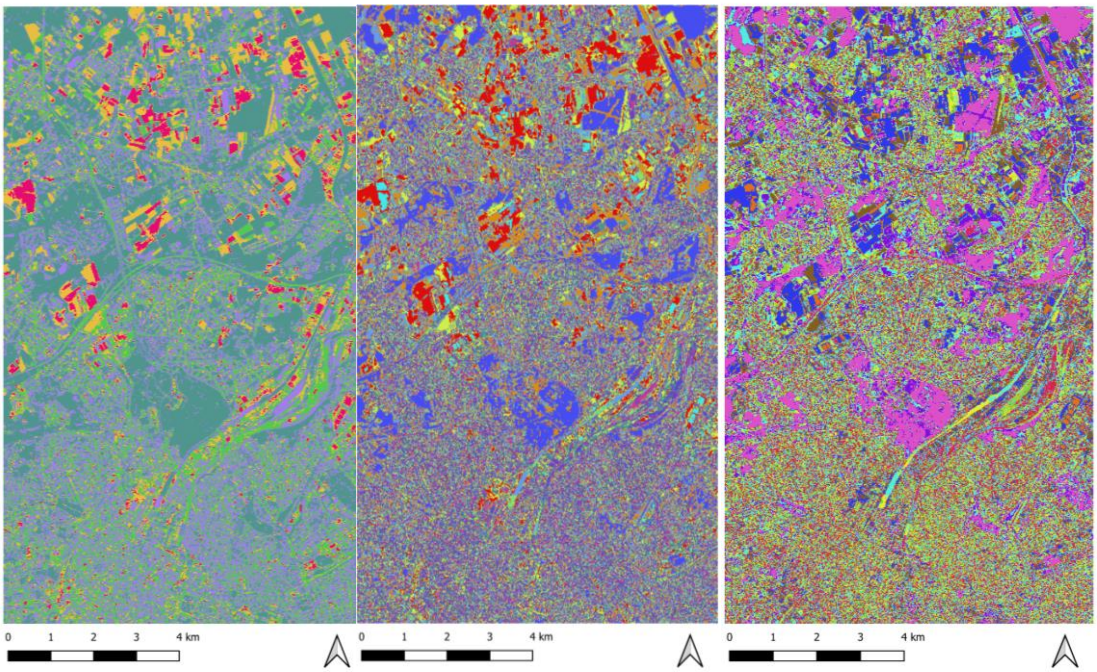

Figure 4: Unsupervised classification maps for summer using different cluster numbers; left: 5 clusters, middle: 10 clusters, right: 20 clusters.

The overall accuracy and kappa hat coefficient for this unsupervised method are globally low, which suggest that better results could be obtained using other classification methods.

3.2. Supervised Classification

The two maps shown in Figure 5 are the final best maps regarding the supervised classification. For both summer and winter images, the Maximum likelihood algorithm obtained the best results because the accuracy assessment output was most accurate compared to the Minimum distance and Spectral angle mapping classification methods (Figure 5). The accuracy assessment will be more elaborated in the next section. The Maximum Likelihood algorithm is the most common classification method, whereby each pixel is assigned to the class having the highest probability. It estimates the means and variances of each class based on the training data and considers of each class the variability of brightness values (Perumal & Bhaskaran, 2010).

While visualizing the classification maps for winter and summer, the maximum likelihood algorithm has the lowest error rate when performing the classification and gives the least “unclassified” pixels. For example, the other two algorithms have difficulties distinguishing the forest from the grassland and the bare soil from arable land. When the land use classification maps for both summer and winter are compared, grassland and forest show a significant drop in winter. It is logical, as most vegetation leaves fall off in winter, so less vegetation is present. Consequently, the spectral signatures will also behave differently. Besides, the coverage of arable land is roughly the same during winter and summer, except that a small part of agricultural land turns into bare soil in winter as fewer crops are produced in low temperatures. This is because we also considered grain fields as arable land in summer, but after the harvest season, part of the harvested fields could turn into bare soil in winter. In general, the natural vegetation (grassland and forest) in winter has decreased compared to summer (Figure 5).

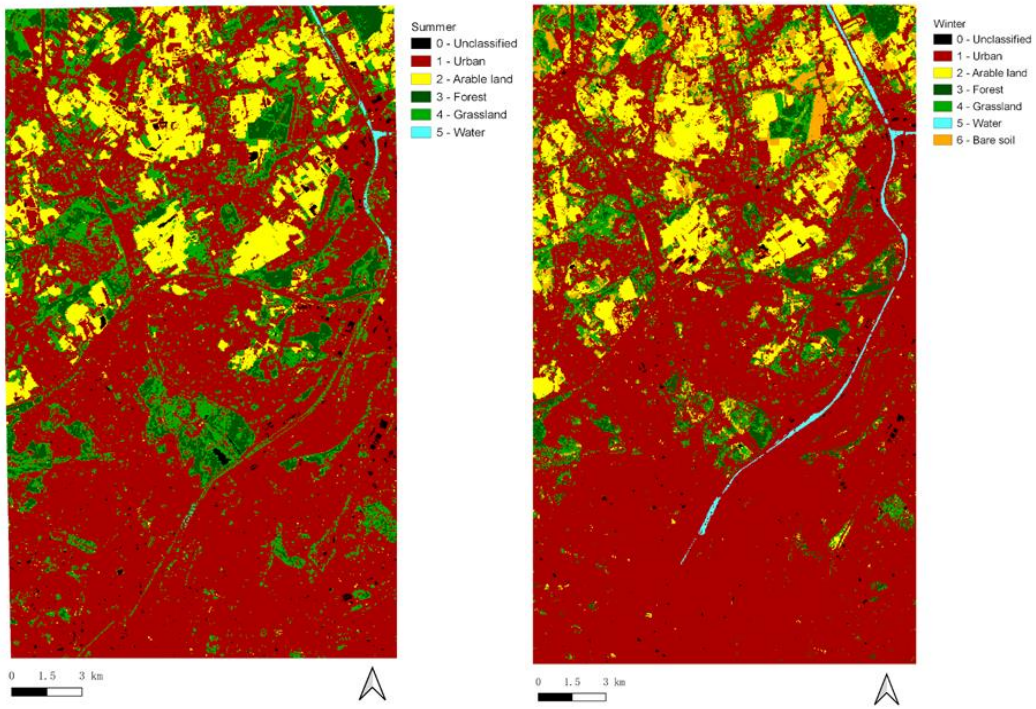

Figure 5: Supervised classification maps in summer (left) and in winter (right).

3.3. Accuracy Assessment

As mentioned in the previous section, the accuracy assessment was applied for the different landcover classification maps. The output results of the best classification are shown in Table 3. The accuracy was defined for each class by combining the overall accuracy (%), the kappa hat (-), the Producer's Accuracy (PA), and the User's Accuracy (UA). The accuracy results are satisfactory, and the overall accuracy and kappa hat are significantly higher for the winter image (84.5%) compared to the summer image (76.4%). A positive kappa hat of 0.58 for summer and 0.69 for winter signifies that the model, and thus also the classification, is better than random (Table 3).

Table 3: The accuracy assessment results for summer and winter landcover classification maps, showing the overall accuracy (%), Kappa hat (-), Producer's Accuracy (PA), and User's Accuracy (UA) for each class.

MC	Image	Summer			Winter		
	Cover	**PA (%)**	**UA (%)**	**Kappa hat**	**PA (%)**	**UA (%)**	**Kappa hat**
1	Urban	96.9	82.5	0.58	98.7	87.0	0.64
2	Arable land	68.9	83.5	0.81	83.6	86.8	0.85
3	Forest	30.4	58.7	0.54	43.0	85.9	0.85
4	Grassland	54.3	54.5	0.47	47.2	70.9	0.66
5	Water	0	-	-	46.8	100.0	1.00
6	Bare soil	-	-	-	65.9	68.1	0.67
	Overall accuracy (%)			76.40			84.5
	Kappa hat (-)			0.58			0.69

There may be several reasons for the high accuracies. By comparing the values of each micro class, shown in Table 3, it is clear that a more detailed subclass classification (for example urban) and larger

land coverage (for example urban and arable land) will improve the classification accuracy. It is the opposite for forest and grasslands, as their spectral signatures are very similar, which makes it easier to cause confusion during the classification. In addition, due to the small extent of the water landcover class in this study area, although its spectral signal is quite different from other micro classes, it is still easy to wrongly classify the pixels. Another reason could be the high variance between the spectral signatures of water. To conclude, it is crucial to classify the micro class reasonably and avoid classifying the land use classes with similar spectral signals into one micro class.

When the accuracy between summer and winter is compared, the winter presents a higher accuracy rate. We can assume that the extra micro class, bare soil, has a contribution to it. Furthermore, it could be that the pixel classification of forest and grassland in summer is not as accurate as in winter. This can also be confirmed by the low PA in summer. The lower UA also means that there is a higher probability of other classes being misclassified into these two. The conclusion was also applicable to the water class for the summer classification. The PA and UA representative water cover areas are almost all misclassified into other classes. Even if the PA of water in winter is not very satisfactory, it is still higher than the PA of summer, which leads to an overall better-classified image assuming 100% PA means a 100 % correct classification.

3.4. Application: air quality in Brussels

To gain insight into the effect of landcover on the air quality in our study area, 3 representative regions with a different land cover were examined further in detail. As introduced before, the qualitative air quality score and corresponding maximal possible deposition maps were calculated and are shown in the following maps (Figure 6, Figure 7). Each figure shows the comparison between the summer and winter images, which gives us the possibility to analyze the temporal effect of the different landcover structures on the air quality.

In Figure 6, the qualitative air quality score maps are shown for winter and summer. In general, a lot of red color is present on both maps because the study area is mostly covered by cities and arable land, and the potential of these landcovers to filter or deposit PM_{10} is very limited. We can conclude that the air quality is generally low, with only a few areas with natural vegetation (forest and grassland) having a good air quality. From a comparison between both maps, it can be concluded that the air quality is reduced from summer to winter. This could be due to the lower extent of vegetated areas in combination with the same extent of urban areas (Figure 6). The same trends are visible in the maximal deposition maps in Figure 7 (Figure 7).

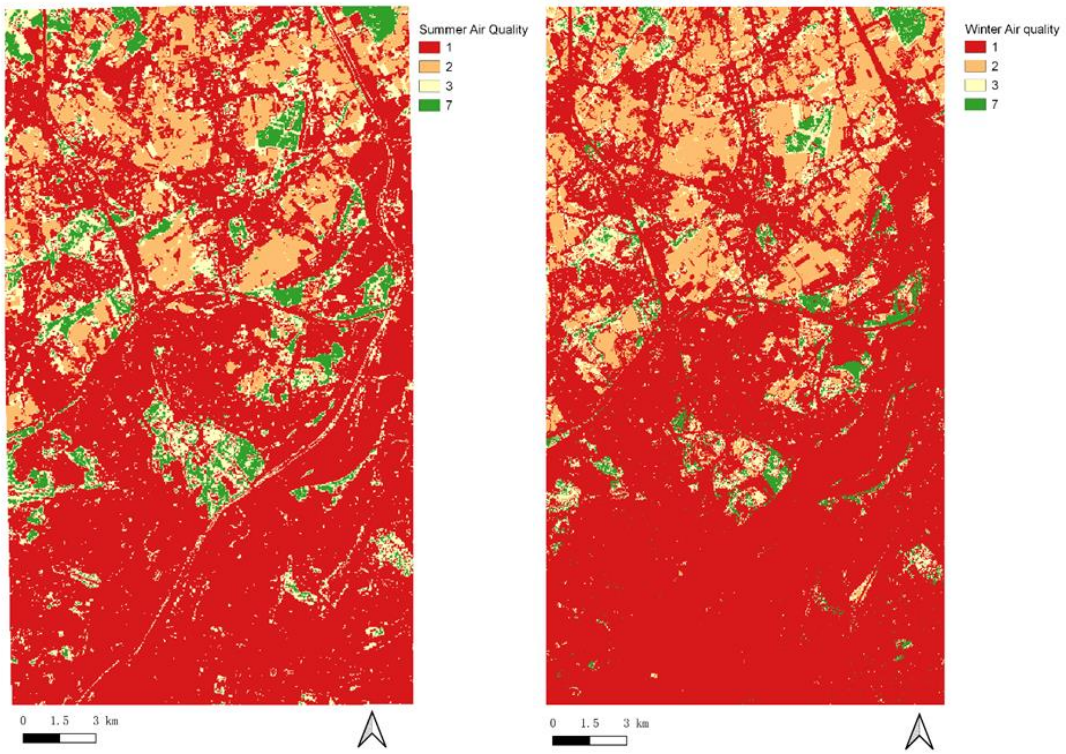

Figure 6: Qualitative air quality score maps in summer (left) and in winter (right).

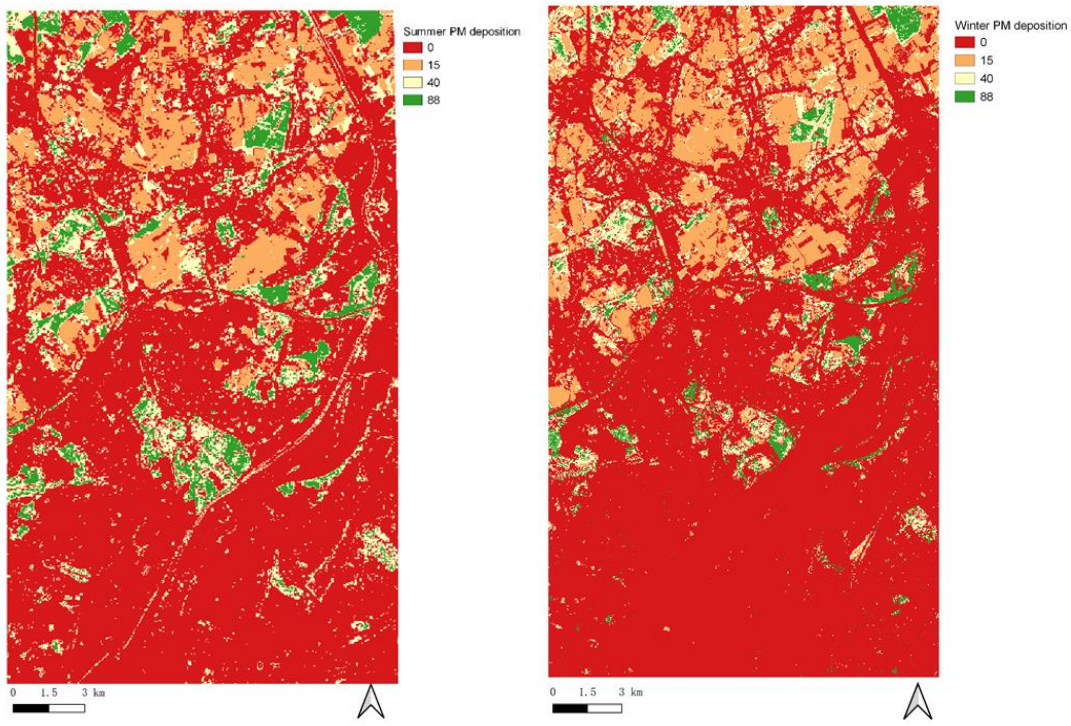

Figure 7: Quantitative maximal deposition maps (in kg PM_{10}/ha) in summer (left) and in winter (right).

Figure 8 shows the general study area and the distribution of the three focus regions. It is worth mentioning that the dominant landcovers in the three regions are different. Region A is located in mainly arable land, region B is predominantly forest and grassland, and region C is located in the urbanized south of the study area. These differences are also visible in the mean values of the air quality scores and PM_{10} depositions for each region separately (Table 4).

Figure 8: The three focus regions located on the summer image, which are Beigem in purple, Laken in blue, and Sint-Joost-Ten-Node in white.

Table 4: The comparison of the mean summer and winter air quality score and the maximal deposition of the focus regions.

REGION	QUALITY SCORE		PM DEPOSITIONS (Kg/Ha)	
	Summer	Winter	Summer	Winter
A (Beigem)	1.71	1.84	10.49	12.01
B (Laken)	2,07	1.58	17.05	9.17
C (Sint-Joost-Ten-Node)	1,04	1.00	0.80	0.04

For region A located in the north, mainly composed of arable land, the total deposit potential for PM_{10} is limited, thus the air quality is low. In the winter, the air quality is slightly higher than in the summer. One reason could be that the bare soil was assumed as arable land during the air quality estimation. However, bare soil has a lower ability to settle dust and particulate matter compared to arable land with crops, which slightly overestimates the winter air quality in this region. As for region B in the center, because it mainly consists of grassland, the air quality is higher than in the other two regions.

However, due to the scattered residential areas inside, the overall air quality is not very satisfactory as well. Especially after the vegetation withered in winter, the air quality is deteriorating very quickly. Finally, for the urbanized region C in the south, the air quality is very worrying, and the high emission in the city makes it even worse. This might be due to the absence of significant land covers, such as forest or grassland, that can deposit dust and particulate matter. In addition, on colder winter days, household heating and vehicle emissions will increase the dust and particulate matter emissions, causing the PM_{10} deposition in the area to drop to a level almost close to zero. The specific values for each region are given in Table 4 (Table 4).

4. Discussion

In general, the supervised classification is more accurate than the unsupervised classification method, as it is confirmed in the overall accuracy and Kappa hat assessment results. The main challenges in achieving high accuracy in unsupervised classification are determining the unknown number of categories in the image and the unknown nature of the categories (Olaode et al., 2014). Correspondingly, because the supervised classification matches the user's class of interest through the comparison between the pixels and the comparison with the known pixels, the user can improve the classification accuracy by selecting an adapted algorithm and defining a suitable class (Perumal and Bhaskaran, 2010). Although the unsupervised classification is not optimal, it remains a useful method and could be combined with the supervised classification method for specific applications (Enderle & Weih, 2005).

Because the study area mainly includes urban cities and suburban areas, the coverage area of the landcover class urban and arable land is very large. Consequently, the coverage area of vegetation that can deposit the dust and particulate matter is low, resulting in a lower air quality level in this area. Besides, the air quality also changes with the seasons, all three focus regions showed worse air quality in winter. If we only look at it from the perspective of visual comparison, this might be due to the lower density of forests and the presence of bare soil that will reduce the filtration capacity. The reason for this phenomenon is not only linked to the different filtering capacities of air pollutants but could also be because the city itself is more likely to form serious air pollution in winter (Samanta et al., 1998). For example, temperature inversion, low wind speed, high vehicle, and domestic emissions often contribute to urban winter pollution. Temperature inversion means that in cold weather, a layer of warm air is pressed between cool air layers, which traps pollution under the clouds and reduces the ability of air movement and particle diffusion. We know that the more frequent coal-fired heating and vehicle use in the winter in the city will lead to a significant increase in pollutant emissions. The low wind speed may promote the accumulation or migration of pollutants, exacerbating the deterioration of air quality (Li et al., 2017). In addition, if the air quality of the three areas of interest is compared, the above conclusions apply here as well. It is found that the air quality in the cities is the worst (region C), followed by the farming area (region A) and the natural vegetation area (region B) in the middle. This region shows a relatively good level, but overall the air quality in the study area is very unsatisfactory.

5. Conclusion

In general, the supervised classification method gave the best results using the Maximum likelihood classifier. In our case, both the summer and winter land use classifications acquired an overall good

accuracy. This is mainly the result of the selection of the easily distinguishable spectral signatures for the different classes (ROI selection). A suitable and representative class classification is crucial as well. For the air quality investigation, it was found that season will definitely affect the air quality levels as the vegetation coverage fluctuates during the year. The air quality is lowest in winter and rises again in summer. This may be caused by the reduction of vegetation coverage, the increase of man-made pollution emissions, and the reduction of air movement and climate influence. At the same time, through the comparison of the three regions, it is concluded that the type of landcover has a correlation with air quality. The air quality is the lowest in the dense urban residential areas, while the areas with more vegetation coverage score relatively better.

6. References

Alkhouri, S. (2015). *Developing spatial information database for the targeted areas*. *December 2014*, 1–23. https://doi.org/10.13140/RG.2.1.2426.1606

Baró, F., Chaparro, L., Gómez-Baggethun, E., Langemeyer, J., Nowak, D. J., & Terradas, J. (2014). *Contribution of ecosystem services to air quality and climate change mitigation policies: The case of urban forests in Barcelona, Spain*. Ambio, *43*(4), 466–479. https://doi.org/10.1007/s13280-014-0507-x

De Craemer, S., Vercauteren, J., Fierens, F., Lefebvre, W., Hooyberghs, H., & Meysman, F. (2020). *CurieuzeNeuzen: monitoring air quality together with 20.000 citizens*. 3–5. https://vito.be/en/atmo-street

Enderle, D. I., & Weih, R. C. J. (2005). *Integrating Supervised and Unsupervised Classification Methods to Develop a More Accurate Land Cover Classification*. Journal of the Arkansas Academy of Science, 59(10). Retrieved from http://scholarworks.uark.edu/jaashttp://scholarworks.uark.edu/jaas/vol59/iss1/10

Humboldt State University. (2019). *Accuracy Metrics*. http://gis.humboldt.edu/OLM/Courses/GSP_216_Online/lesson6-2/metrics.html

Lefebvre, W., Janssen, S., Vankerkom, J., Deutsch, F., Veldeman, N., & Fierens, F. et al. (2011). *Making High Resolution Air Quality Maps for Flanders, Belgium*. Air Pollution Modeling And Its Application XXI, 205-211.

Li, L., Yan, D., Xu, S., Huang, M., & Wang, X. (2017). *Characteristics and source distribution of air pollution in winter.* Environmental Pollution, 44–53. https://doi.org/10.1016/j.envpol.2016.12.037

Meysman, F. J. R., & De Craemer, S. (2018). *CurieuzeNeuzen Vlaanderen: Het cijferrapport*. 1–56. http://www.standaard.be/curieuzeneuzen

Olaode, A., Naghdy, G. A., & Todd, C. (2014). *Unsupervised Classification of Images : A Review*. September.

Perumal, K., & Bhaskaran, R. (2010). *Supervised Classification Performance of Multispectral Images*. *2*(2), 124–129. http://arxiv.org/abs/1002.4046

Samanta, G., Chattopadhyay, G., Mandal, B.K., Chowdhury, T.R., Chowdhury, P.P., Chanda, C.R., Banerjee, P., Lodh, D., Das, D., Chakraborti, D. (1998). *Air pollution in Calcutta during winter – A three-year study*. Current Science Associaton, 75(2), 123–138

Singh, N. (2020). *What is K-Means Clustering? - Artificial Intelligence in Plain English*. Artificial Intelligence. Retrieved December 21, 2021, from https://ai.plainenglish.io/what-is-k-means-clustering-3060791cb589

Walton, A., Mohammad, D.-I., Tourian, J., & Omid Elmi, M. S. (2015). *Assessing the performance of different classification methods to detect inland surface water extent*. University of Stuttgart